

## Parameters of Native Silver Formation in the Ag–Fe–S System Based on the EMF Determination at 518–728 K and 1–5000 Bar Total Pressure

D. A. Chareev<sup>a</sup>, E. G. Osadchii<sup>b</sup>, Yu. B. Shapovalov<sup>b</sup>,  
Corresponding Member of the RAS N. S. Bortnikov<sup>a</sup>, and N. N. Zhdanov<sup>b</sup>

Received April 17, 2006

DOI: 10.1134/S1028334X06080162

Pyrite (FeS<sub>2</sub>) and pyrrhotite (Fe<sub>1-x</sub>S) often occur at Ag-bearing ore occurrences and deposits with native silver (Ag) or acanthite (Ag<sub>2</sub>S), a low-temperature modification of argentite. Intergrowths of these minerals were established, for example, in pyrite samples from the Texas Gulf Sulfur's Kidd Creek deposit, Timmons, Ontario [1].

The significant (~20%) positive volumetric effect of the reaction between pyrrhotite and argentite with the formation of pyrite and native silver is, probably, the greatest effect for metal–sulfide equilibria. As a result, a 5000 bar pressure on solid phases increases the temperature of native silver formation approximately by 50 K [1]. Hence, the pyrite–pyrrhotite–argentite–silver assemblage may be considered a potential geobarometer.

The phase relations in the Ag–Fe–S system have been studied with the method of solid-phase annealing at the pressure of natural vapor [1]. The metallic silver–pyrite assemblage is stable below 521 ± 8 K. At a higher temperature, this assemblage gives way to the argentite–pyrrhotite–pyrite assemblage, but phase relations remain principally unchanged up to 805 K. Less than 0.1 at % of Ag can dissolve from sulfides and argentite. The Fe<sub>1-x</sub>S compositions in the Ag<sub>2</sub>S + 'FeS' + FeS<sub>2</sub> assemblage at >521 ± 8 K are identical to those in the binary 'FeS' + FeS<sub>2</sub> assemblage [2, 3].

The phase relations in which we are interested in the Ag–Fe–S system are described with a solid-phase reaction



where all phases except pyrrhotite occur in the standard state (their activity is equal to unity).

Reaction (1) was realized in the completely solid galvanic cell



with a common gas space in argon atmosphere.

The electromotive force (EMF) of the cell is related to the free energy of the reaction by the equation

$$\Delta G = -n \cdot 10^{-3} \cdot F \cdot E, \quad (2)$$

where  $\Delta G$  is the free energy of reaction (1);  $n$  is the number of electrons that participate in the electrochemical process ( $n = 2$  for reaction (1));  $F = 96\,484.56 \text{ C} \cdot \text{mol}^{-1}$  is the Faraday constant; and  $E$  is the EMF of the galvanic cell, mV.

Zero EMF of the cell ( $E(\text{A}) = 0$ ) corresponds to the equality of the chemical potentials of silver in both parts of the cell or, in other words, to the formation of metallic silver in the system at a constant pressure (four-phase assemblage).

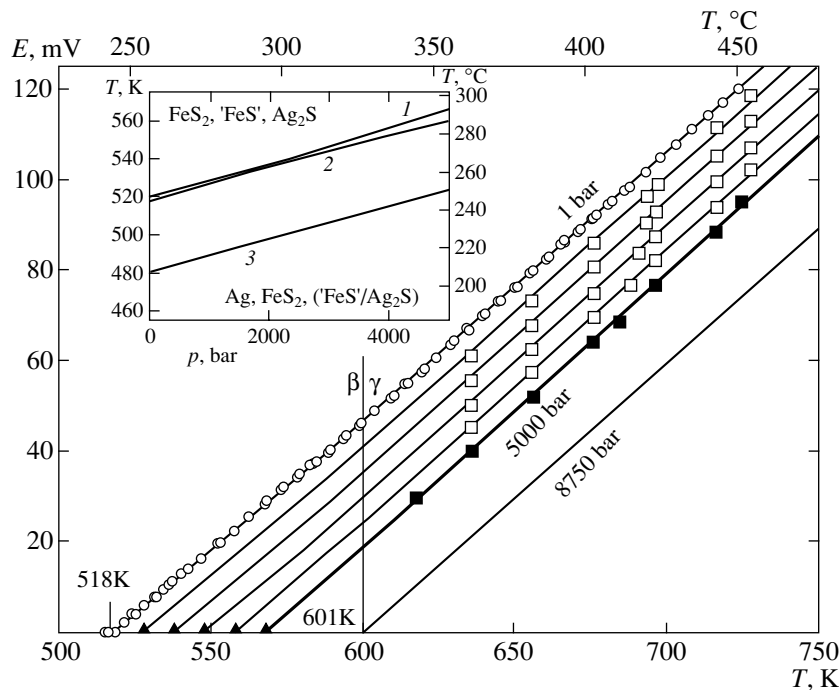
The pyrite–pyrrhotite mixture was synthesized in several stages in evacuated (~10<sup>-4</sup> bar) ampules made of quartz glass. The sample system (working electrode) was prepared as a mixture of 'FeS', FeS<sub>2</sub>, and Ag<sub>2</sub>S in a molar proportion of 1: 1: 1 and approximately 400 mg in mass. This mixture was pressed into pellets 6 mm in diameter under a load of 1.0–1.2 t. The design of the cell and EMF measurement method are described in [4].

The experiments at atmospheric pressure in the argon atmosphere were carried out previously [5] with temperature titration, i.e., by setting a constant equilibrium EMF value at a given temperature. Equilibrium was deemed to be achieved when the EMF values and temperature remained ±0.02 mV and ±0.15 K, respectively, over a few hours (sometimes, days).

The experiment at high gas pressure does not differ principally from that at atmospheric pressure or at the pressure of natural vapor in vacuum. The study at

<sup>a</sup> Institute of Geology of Ore Deposits, Petrography, Mineralogy, and Geochemistry, Russian Academy of Sciences, Staromonetnyi per. 35, Moscow, 119017 Russia; e-mail: charlic@mail.ru

<sup>b</sup> Institute of Experimental Mineralogy, Russian Academy of Sciences, Chernogolovka, Moscow oblast, 142432 Russia



Experimental relationship of cell (A) EMF vs. temperature. Circles are experimental points obtained at atmospheric pressure. Deviations of experimental points from the calculated isobars are apparent, because the pressures are slightly distinct from those divisible by 1000. The inset demonstrates the relationship of the stability temperature of four-phase assemblage vs. total pressure. (1) Experimental data, Eq. (9); (2) calculation for the four-phase assemblage with participation of troilite (FeS) [9]; (3) calculation for the four-phase assemblage with participation of monoclinic pyrrhotite ( $\text{Fe}_7\text{S}_8$ ) [9].

1000–5000 bar was performed in a high-pressure vessel [6] that allows working under high  $pT$  conditions (up to 10 kbar and 1400 K, respectively). Commodity argon from a gas cylinder without additional refinement was used as a pressure-transmitting medium.

The temperature, pressure, and EMF were measured with a universal, multichannel high-precision digital device attached to a PC [7]. The measurement accuracy was  $\pm 0.005$  mV (range 0–16 mV) for the temperature channel and  $\pm 0.03$  mV (range 0–500 mV) for the EMF channel. The input resistance of the channels for EMF measurements was  $10^{12}$ – $10^{13}$   $\Omega$ . The cell temperature was measured with a chromel–alumel thermocouple at atmospheric pressure and with a Pt/Pt (10 wt % Rh) thermocouple in the high-pressure vessel. The pressure was determined by readings of a D-1000 strain meter, which was calibrated to 2000 bar with a deadweight pressure tester. The error of measurements ( $2\sigma$ ) was 3 bar, and sensitivity was not worse than 1 bar. Thus, the uncertainty of pressure determination within a range of 1–5000 bar was not higher than 10 bar.

The experiments in the high-pressure vessel were carried out with temperature titration: the pressure was changed approximately by 1000 bar after the establishment of equilibrium EMF at a given temperature; in so doing, we assumed that the given temperature and constant EMF are retained. The temperature is a limiting factor of equilibrium, while the equilibrium response of

the potential of the cell to the change in pressure was practically instantaneous. The duration of controlling the measurements at each pressure after achievement of temperature equilibrium was no less than 60 min.

The figure presents the results of measurements in cell (A) at atmospheric pressure (more than 130 points with a step of 5 K) as two linear equations ( $\Delta_r C_p = 0$ ) that correspond to the stability field of high-temperature ( $\gamma$ ) and low-temperature ( $\beta$ ) pyrrhotite in reaction (1):

$$E(A, \gamma), (\text{mV}) = -(311.7 \pm 1.1) + (0.5968 \pm 0.0017) \cdot T, \quad (601 < T(\text{K}) < 723), \quad (3)$$

$$R^2 = 0.9999,$$

$$E(A, \beta), (\text{mV}) = -(290.9 \pm 1.4) + (0.5621 \pm 0.0025) \cdot T, \quad (518 < T(\text{K}) < 601), \quad (4)$$

$$R^2 = 0.9998.$$

The errors in the experimental data were determined with the least square method for a  $2\sigma$  confidence interval.

The temperature of the type 1 phase transition  $T_{\beta\gamma} = 601 \pm 2$  K is determined from the joint solution of Eqs. (3) and (4). The enthalpy of the phase transition is  $\Delta_{\beta\gamma}H = -2F(\partial\Delta E(A)/\partial T)_p \cdot T_{\beta\gamma} = 4020 \pm 200$  J  $\cdot$  mol $^{-1}$ .

It is known that the composition and activity of pyrrhotite on the pyrite–pyrrhotite equilibrium line virtu-

ally do not depend on pressure [3]. Hence, the temperature and thermal effect of phase transition in pyrrhotite do not depend (at a first approximation) on pressure as well.

The equilibrium in cell (A) was established very rapidly and is reproducible within the entire studied  $T$ - $p$  range. It is probably explained by the presence of silver sulfide, which is an ionic conductor with semiconductor properties [8]. The relatively high mobility of Ag ions and electron conduction promote the fast establishment of equilibrium between pyrrhotite, pyrite, and  $\text{Ag}_2\text{S}$ .

The instant equilibrium response of EMF to pressure changes at a constant temperature confirms that the composition and activity of FeS in pyrrhotite are independent of pressure.

The accuracy of experimental data obtained at atmospheric pressure is definitely higher than the accuracy of the results obtained in the high-pressure vessel owing to the smaller number of points and shorter time assigned to the establishment of equilibrium. Thus, the relationship  $E(T, 1 \text{ atm})$  (3) was chosen as the basic one for the determination of functional relationships between EMF versus temperature and pressure. The effect of pressure on the EMF of the cell was found as an additional function  $c_r \cdot (p - 1)$ , where  $c_r$  is related to variation of the molar volume of reaction (1) by equations

$$\begin{aligned} c_r \cdot (p - 1) &= E(T, p) - E(T, 1 \text{ atm}) \\ &= -\Delta_r V_m(T, p) \cdot (p - 1) / n \cdot F. \end{aligned} \quad (5)$$

In the general case,  $\Delta_r V_m$  is a function of temperature and pressure. The thermal and baric coefficients for all phases in reaction (1) are unknown. For relatively low pressure and temperature,  $\Delta_r V_m(1)$  may be assumed, at a first approximation, as a constant and this assumption is commonly accepted for estimation of the pressure effect. In our experiment, the integral effect of pressure was determined in situ and the accuracy of the experimental data on  $\Delta_r V_m(1)$  obtained at a pressure is a priori not worse than the accuracy of the reference data on  $\Delta_r V_m(1)$  for normal conditions.

The coefficients of the equation

$$E(T, p) = a + bT + c_r(T, p) \cdot (p - 1), \quad (6)$$

where  $c_r(T, p)$  is a constant, may be found in several ways. To calculate this coefficient, we used only the experimental points  $(E, T, p)$  obtained at a pressure of about 5000 bar. As a result, a numerical relationship between EMF, temperature, and total pressure has been obtained for reaction (1) in the field of  $\gamma$ -pyrrhotite stability:

$$\begin{aligned} E(A, \gamma)(T, p)(\text{mV}) &= \\ &= -311.7 + 0.5968 \cdot T - 5.343 \cdot 10^{-3} \cdot (p - 1). \end{aligned} \quad (7)$$

The double root of the mean-square deviation ( $2\sigma$ ) of the experimental data from the analytical relationship is 1.3 mV, which corresponds to an uncertainty of 2 K or 180 bar.

In the EMF versus temperature plot (figure), the experimental data are supplemented by  $E(T)$  relationships calculated for pressures of 1000, 2000–5000, and 8750 bar from Eq. (7). The figure also shows the EMF-temperature relationship for reaction (1) at 1 atm as Eqs. (2) and (3), as well as all experimental points.

The lines of  $E(T)$  dependence for the pressure values divisible by 1000 atm were extrapolated to the field below the temperature of  $\beta$ - $\gamma$  transition in pyrrhotite. If we assume that the temperature and enthalpy of this transition do not depend on pressure, the relationship  $E(T, p)$  at a temperature below 601 K may be obtained by substitution of the relevant side of Eq. (3) in Eq. (7) by Eq. (4):

$$\begin{aligned} E(A, \beta)(T, p)(\text{mV}) \\ &= -290.9 + 0.5621 \cdot T - 5.343 \cdot 10^{-3} \cdot (p - 1). \end{aligned} \quad (8)$$

The temperature values at which metallic silver starts to form depending on pressure are shown by triangles. Equations (9) and (10) also indicate the pressure ( $p_4$ ), at which the four-phase assemblage  $E(T, p) = 0$  exists depending on temperature:

$$\begin{aligned} (p_4(\beta) - 1) &= 105.21 \cdot (T - 517.5), \\ &(518 < T(\text{K}) < 601), \end{aligned} \quad (9)$$

$$(p_4(\gamma) - 1) = 111.69 \cdot (T - 522.3), \quad (T(\text{K}) > 601). \quad (10)$$

Equation (9) is applicable to the calculation of the pressure at which the four-phase assemblage with the participation of  $\beta$ -pyrrhotite exists at a temperature below  $601 \pm 2$  K, while Eq. (10) is used for calculation of  $p_4$  at a temperature above 601 K in the four-phase assemblage with  $\gamma$  pyrrhotite. When the pyrite- $\gamma$ -pyrrhotite-argentite assemblage is cooling at a pressure of  $8750 \pm 180$  bar, the phase transition of pyrrhotite coincides with onset of metallic silver formation.

The  $T$ - $p$  relationships of metallic silver formation were also calculated for the troilite (FeS) + pyrite + argentite + silver and the monoclinic pyrrhotite ( $\text{Fe}_7\text{S}_8$ ) + pyrite + argentite + silver assemblages in order to compare the results with experimental data. All values for these calculations were taken from handbook [9]. The temperatures of metallic silver formation  $T_4$  ( $p = 1$  atm) in our experiment and in the calculation with the participation of troilite virtually coincide at atmospheric pressure. However, the experimental line has a steeper slope. By comparison, the change in the standard molar volume is  $0.7906 \pm 0.005 \text{ J} \cdot \text{bar}^{-1}$  for the reaction with the participation of stoichiometric pyrrhotite and  $0.9036 \pm 0.006 \text{ J} \cdot \text{bar}^{-1}$  for the reaction with the participation of monoclinic pyrrhotite. At the same time, the change of the molar volume for the studied reaction (1)

calculated from Eqs. (7) and (8) is  $1.031 \pm 0.09 \text{ J} \cdot \text{bar}^{-1}$  (inset in figure).

Thus, if the temperature of native silver formation in association with iron sulfide(s) may be established independently, for example, from fluid inclusions, the experimentally obtained Eqs. (9) and (10) may be used as geobarometers. Thereby, it must be kept in mind that silver is stable at any pressure at a temperature below 518 K.

The established kinetic attributes of these reactions have self-dependent implications for experimental studies. The occurrence of silver sulfide as one of the phases of the sample system (electrode) of a galvanic cell accelerates the achievement of equilibrium and thus substantially widens the temperature range of investigations. The high accuracy, relative simplicity, and possibility to control the achievement of equilibrium during the run are also obvious advantages of the EMF method.

#### ACKNOWLEDGMENTS

We thank N.I. Bezmen for providing the high-pressure vessel and A.P. Tarasov for assistance in conducting the experiments.

This work was supported by the Russian Foundation for Basic Research (project nos. 05-05-64237 and 06-05-64444) and the Earth Sciences Division of the Russian Academy of Sciences (program no. 7).

#### REFERENCES

1. L. A. Taylor, *Mineral. Deposita* **5**, 41 (1970).
2. R. G. Arnold, *Econ. Geol.* **57**, 72 (1962).
3. P. Toulmin, III and P. B. Barton, Jr., *Geochim. Cosmochim. Acta* **28**, 641 (1964).
4. E. G. Osadchii and O. A. Rappo, *Am. Mineral.* **89**, 1405 (2004).
5. D. A. Chareev and E. G. Osadchii, *Proceedings of All-Russia Scientific Conference "New Ideas in Earth Sciences"* (Moscow, 2005), Vol. 2, p. 100 [in Russian].
6. G. G. Likhoidov and G. N. Chernysheva, in *Modern Equipment and Methods of Experimental Mineralogy* (Nauka, Moscow, 1985), pp. 116–121 [in Russian].
7. N. N. Zhdanov, E. G. Osadchii, and A. V. Zotov, in *Proceedings of XV Russian Conference on Experimental Mineralogy* (Moscow, 2005), p. 166.
8. S. Miyatani, *J. Phys. Soc. Japan* **24**, 328 (1964).
9. R. A. Robie and B. S. Hemingway, *US Geol. Survey Bull.*, No. 2131, 1995.